

The Uptake of Apoptotic Cells Drives *Coxiella burnetii* Replication and Macrophage Polarization: A Model for Q Fever Endocarditis

Marie Benoit, Eric Ghigo, Christian Capo, Didier Raoult, Jean-Louis Mege*

Unité de Recherche sur les Maladies Infectieuses Transmissibles et Emergentes, CNRS UMR 6236, Institut Fédératif de Recherche 48, Université de la Méditerranée, Faculté de Médecine, Marseille, France

Abstract

Patients with valvulopathy have the highest risk to develop infective endocarditis (IE), although the relationship between valvulopathy and IE is not clearly understood. Q fever endocarditis, an IE due to *Coxiella burnetii*, is accompanied by immune impairment. Patients with valvulopathy exhibited increased levels of circulating apoptotic leukocytes, as determined by the measurement of active caspases and nucleosome determination. The binding of apoptotic cells to monocytes and macrophages, the hosts of *C. burnetii*, may be responsible for the immune impairment observed in Q fever endocarditis. Apoptotic lymphocytes (AL) increased *C. burnetii* replication in monocytes and monocyte-derived macrophages in a cell-contact dependent manner, as determined by quantitative PCR and immunofluorescence. AL binding induced a M2 program in monocytes and macrophages stimulated with *C. burnetii* as determined by a cDNA chip containing 440 arrayed sequences and functional tests, but this program was in part different in monocytes and macrophages. While monocytes that had bound AL released high levels of IL-10 and IL-6, low levels of TNF and increased CD14 expression, macrophages that had bound AL released high levels of TGF- β 1 and expressed mannose receptor. The neutralization of IL-10 and TGF- β 1 prevented the replication of *C. burnetii* due to the binding of AL, suggesting that they were critically involved in bacterial replication. In contrast, the binding of necrotic cells to monocytes and macrophages led to *C. burnetii* killing and typical M1 polarization. Finally, interferon- γ corrected the immune deactivation induced by apoptotic cells: it prevented the replication of *C. burnetii* and re-directed monocytes and macrophages toward a M1 program, which was deleterious for *C. burnetii*. We suggest that leukocyte apoptosis associated with valvulopathy may be critical for the pathogenesis of Q fever endocarditis by deactivating immune cells and creating a favorable environment for bacterial persistence.

Citation: Benoit M, Ghigo E, Capo C, Raoult D, Mege J-L (2008) The Uptake of Apoptotic Cells Drives *Coxiella burnetii* Replication and Macrophage Polarization: A Model for Q Fever Endocarditis. PLoS Pathog 4(5): e1000066. doi:10.1371/journal.ppat.1000066

Editor: Frederick M. Ausubel, Massachusetts General Hospital, United States of America

Received: February 22, 2008; **Accepted:** April 11, 2008; **Published:** May 16, 2008

Copyright: © 2008 Benoit et al. This is an open-access article distributed under the terms of the Creative Commons Attribution License, which permits unrestricted use, distribution, and reproduction in any medium, provided the original author and source are credited.

Funding: This work was supported by the «crédits ministériels du Programme Hospitalier de Recherche Clinique» (PHRC 2005) obtained for the «Immunodépression de la fièvre Q : rôle des cellules régulatrices et de l'apoptose» and the «Fondation pour la Recherche Médicale».

Competing Interests: The authors have declared that no competing interests exist.

* E-mail: Jean-Louis.Mege@medecine.univ-mrs.fr

Introduction

Infective endocarditis (IE) has long been recognized as a fatal disease. Despite the availability of antimicrobial agents and cardiac surgery, IE still causes high morbidity and mortality. About 75% of patients with IE have pre-existing cardiac diseases [1], including congenital cardiac malformations, acquired valvular dysfunction and prosthetic cardiac valves [2]. Normal endocardium is resistant to colonization by bacteria [3] unless it exhibits pre-existing lesions. Lesions expose underlying extracellular matrix proteins and enable deposition of fibrin-platelet clots [4], bacterial adhesion [5] and recruitment of monocytes, which produce tissue factor and inflammatory cytokines [6]: this usually leads to the growth of vegetation. Cardiac valve lesions are associated with pathological fluid shear stress [7]. In vitro, fluid shear stress modifies the structure and the function of the endothelium [8] and increases apoptosis of neutrophils [9], platelets [10] and monocytes (Mo) [11], suggesting that leukocyte apoptosis may be related to cardiac valvulopathy.

IE associated with negative blood culture constitutes 5% of all IE cases. It is often caused by obligate intracellular pathogens, such as *Coxiella burnetii* [12]. This bacterium that resides in Mo and

macrophages [13] is the agent of the so-called Q fever. In patients with acute Q fever and valve disease, chronic endocarditis will develop in 30% to 50% of cases [14]. Q fever endocarditis is characterized by the lack of vegetations [15] and granuloma formation and impaired systemic cell-mediated immune response [13], whereas acute Q fever is usually controlled by the cell-mediated immune system [13], including the interferon (IFN)- γ pathway [16,17]. This suggests that mechanisms distinct from endothelial lesions are involved in the immune impairment associated with the development of Q fever endocarditis. It is tempting to speculate that leukocyte apoptosis induced by cardiac valvulopathy may impair the immune response to *C. burnetii* through the modulation of macrophage polarization induced by the binding of apoptotic cells. Indeed, the phagocytosis of apoptotic cells by phagocytes and neighboring cells results in a powerful anti-inflammatory and immunosuppressive response [18] via the secretion of anti-inflammatory molecules, such as interleukin (IL)-10 and transforming growth factor (TGF)- β 1 [19]. Different activation states of macrophages induced by microbial products, cytokines, glucocorticoids or immune complexes have been described [20]. By referring to the Th1/Th2

Author Summary

Infective endocarditis (IE) is a problem of public health that still causes high mortality despite antibiotic treatments. Most of the patients who develop an IE have pre-existing cardiac lesions, although the relationship between IE and valvulopathy is not clearly understood. We showed here that patients with valvulopathy exhibited increased levels of circulating apoptotic leukocytes. As the binding of apoptotic cells to monocytes and macrophages is known to inhibit their inflammatory activity, we hypothesized that the high levels of circulating apoptotic leukocytes may be responsible for the immune impairment observed in Q fever endocarditis, an IE due to *Coxiella burnetii*, a bacterium that survives in monocytes and macrophages. The binding of apoptotic lymphocytes to monocytes and macrophages increased the replication of *C. burnetii* by stimulating their anti-inflammatory response. In contrast, the binding of necrotic lymphocytes to monocytes and macrophages induced *C. burnetii* killing and stimulated an inflammatory response. Interferon- γ , which is associated with the control of *C. burnetii* infection, prevented the replication of *C. burnetii* in monocytes and macrophages that have bound apoptotic lymphocytes by stimulating their inflammatory response. In conclusion, we suggest that leukocyte apoptosis associated with valvulopathy may be critical for the pathogenesis of Q fever endocarditis by deactivating immune cells and creating a favorable environment for pathogen persistence.

nomenclature, many now refer to M1 and M2 macrophages. M1 macrophages, stimulated by lipopolysaccharide (LPS) and/or IFN- γ , have a high capacity for antigen presentation, express CCR7, exhibit high levels of inducible nitric oxide synthase (iNOS) and secrete inflammatory cytokines, such as tumor necrosis factor (TNF), IL-1, IL-6 and IL-12, and chemokines, such as CXCL8, CCL2 and CCL5. M2 macrophages, induced by IL-4, IL-13 or IL-10, express the Fc γ -receptor type 2 (Fc γ -R2, CD23), the mannose receptor (MR) and CD14 and secrete anti-inflammatory cytokines, such as IL-10, TGF- β 1 and IL-1 receptor antagonist (IL-1ra), and specific chemokines, such as CCL16, CCL18 and CCL24 [21]. The expression of arginase-1 by M2 macrophages shifts L-arginine metabolism toward the production of ornithine and polyamines by arginase-1, which, in turn, contributes to blocking the iNOS pathway [22].

The aim of this study was to determine the mechanisms by which valvulopathy creates favorable conditions for the establishment of Q fever endocarditis. We showed that apoptosis of circulating leukocytes was increased in patients with valvulopathy, independently of Q fever. We also showed that the binding of apoptotic lymphocytes (AL) by Mo and Mo-derived macrophages (MDM) increased *C. burnetii* replication and polarized Mo and MDM toward a M2 profile. Interestingly, IFN- γ prevented *C. burnetii* replication and re-directed Mo and MDM toward a M1 program. Leukocyte apoptosis associated with valvulopathy may be critical in the pathogenesis of IE by creating a favorable environment for pathogen persistence through the deactivation of immune competent cells.

Results

Circulating apoptosis markers in patients with valvulopathy

Apoptosis was investigated by measuring circulating nucleosomes and caspase activity in leukocytes from control subjects,

patients with valvulopathy and patients with Q fever (Figure 1). In patients with valvulopathy, acute Q fever and valvulopathy or Q fever endocarditis, circulating nucleosomes (Figure 1A) and the percentage of active caspases in leukocytes (Figure 1B–F) significantly ($p < 0.001$) increased as compared to control subjects. Interestingly, circulating nucleosomes ($p < 0.001$) and the percentage of active caspases in leukocytes ($p < 0.01$) was significantly higher in patients with acute Q fever and valvulopathy than in patients with acute Q fever without valvulopathy. These results showed that patients with valvulopathy exhibited increased levels of apoptotic leukocytes.

To determine which type of leukocytes was apoptotic, cells with active caspases were quantified in CD3- and CD14-gated populations (Figure 1G). In patients with valvulopathy, with or without acute Q fever, the percentages of CD3 $^+$ and CD14 $^+$ cells that expressed active caspases were significantly higher ($p < 0.01$) as compared to control subjects and patients with acute Q fever without valvulopathy. They were similar to those found in patients with Q fever endocarditis (Figure 1G). Taken together, these results show that increased leukocyte apoptosis was associated with valvulopathy.

Binding of apoptotic lymphocytes to monocytes and macrophages

Impaired immune responses associated with Q fever endocarditis may result from the binding of apoptotic cells to professional phagocytes. Consequently, we created an experimental model to test *in vitro* this hypothesis. Apoptosis of lymphocytes was induced by 10^{-6} M dexamethasone, which stimulated apoptosis via a caspase-dependent pathway (Figure S1). As a control, necrosis of lymphocytes was induced by a 95°C shock (Figure S1).

As apoptotic cells stimulates cytoskeleton reorganization in phagocytic cells [23], we analyzed the morphological changes induced by AL and necrotic lymphocytes (NL) in Mo (Figure 2A) and MDM (Figure 2B). Resting Mo and MDM were rounded and did not present ruffles or filopodia. The F-actin distribution was roughly homogeneous in quiescent Mo and MDM. AL induced intense morphological changes consisting of membrane ruffles in Mo and MDM. In contrast to AL, NL induced the formation of numerous filopodial extensions in Mo and MDM. F-actin was redistributed around membrane ruffles and filopodial extensions induced by AL and NL, respectively. The percentage of Mo and MDM with membrane ruffles or filopodia was quantified: AL induced membrane ruffles in about 70% of Mo (Figure 2C) and MDM (Figure 2D) whereas NL induced filopodia in about 75% of Mo (Figure 2C) and MDM (Figure 2D). These results showed that AL and NL induced distinct cytoskeleton reorganization in Mo and MDM.

Finally, we determined the time course of AL and NL binding. The binding of AL and NL to Mo and MDM was maximal after 2 h. Indeed, about 80% of Mo (Figure 2E) and MDM (Figure 2F) had bound at least one AL or NL after 2 h. Thus, a 2-h incubation time of AL and NL with Mo and MDM was used in further experiments.

Effect of apoptotic lymphocyte binding on the intracellular fate of *C. burnetii*

Mo and MDM were incubated with AL or NL for 2 h and infected with *C. burnetii*. The binding of AL and NL to Mo (Figure 3A, inset) and MDM (Figure 3B, inset) had no effect on *C. burnetii* phagocytosis. *C. burnetii* survived without replication in control Mo (Figure 3A) and moderately replicated in control MDM (Figure 3B), as determined by real-time quantitative PCR

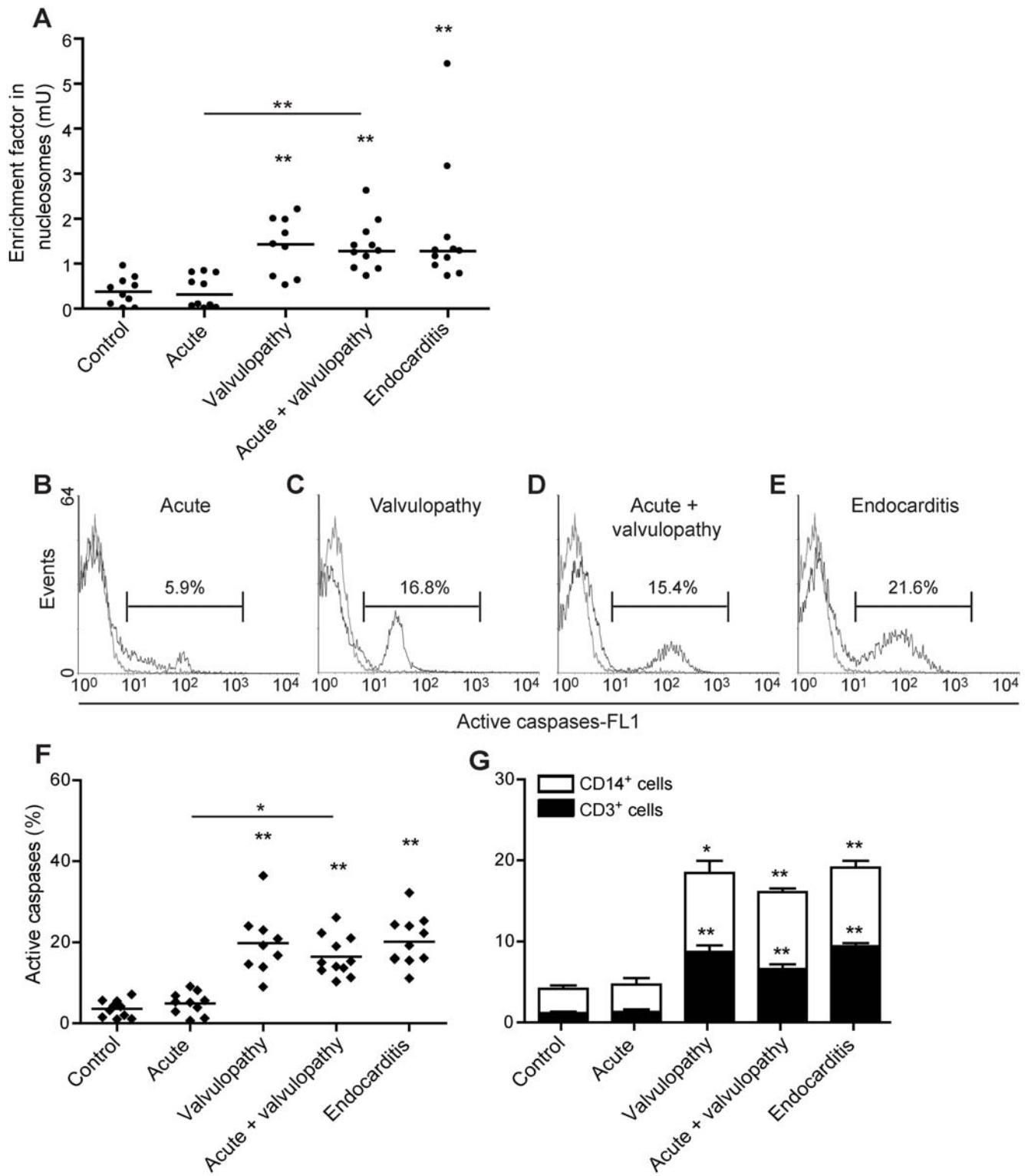


Figure 1. Circulating apoptosis markers in patients with valvulopathy. A, The circulating levels of nucleosomes was determined by immunoassays in control subjects, patients with acute Q fever, valvulopathy, acute Q fever with valvulopathy and Q fever endocarditis. Results are expressed as individual values with medians. B–E, Active caspases were detected through FLICA fluorescence (FL1 channel) and flow cytometry analysis of leukocytes from patients with acute Q fever (B), valvulopathy (C), acute Q fever with valvulopathy (D) and Q fever endocarditis (E) compared to control subjects (gray line). F, The results are expressed as percentage of active caspases for each individual. Bars represent the median of the values. G, Active caspases were quantified in CD3⁺ and CD14⁺ leukocytes from control subjects and patients. The results represent the mean \pm SEM. * $p < 0.01$ and ** $p < 0.001$. doi:10.1371/journal.ppat.1000066.g001

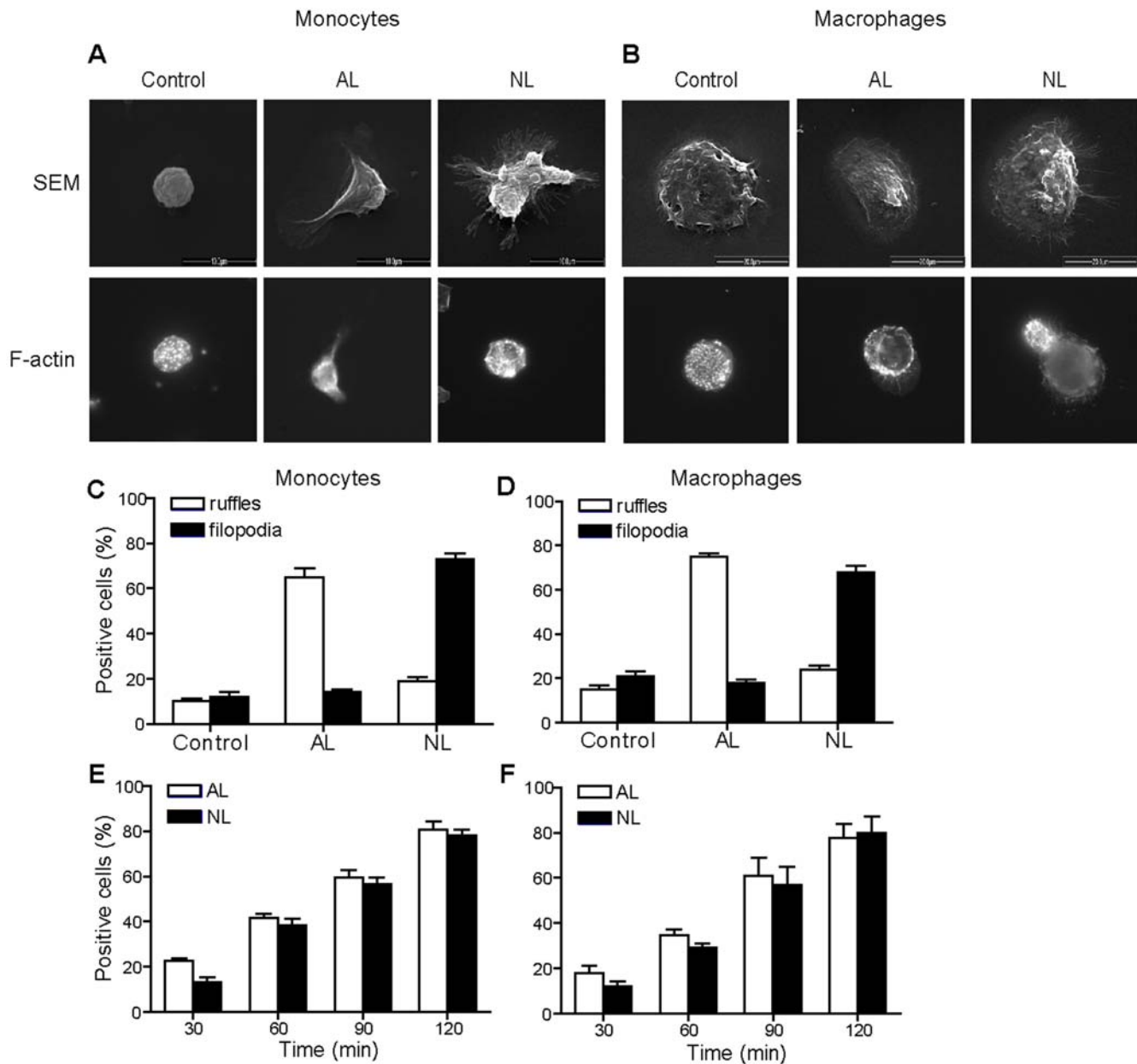


Figure 2. Binding of AL and NL to Mo and MDM. A and B, Mo (A) and MDM (B) were incubated with AL and NL for 30 min. Mo and MDM were fixed, gold-coated and analyzed by SEM or labeled with BODIPY phalloidin and observed in fluorescence microscopy. Representative micrographs are shown. C and D, the percentage of Mo (C) and MDM (D) that exhibited membrane ruffles or spikes was determined by fluorescence microscopy. E and F, Fluorescent AL and NL were incubated with Mo and MDM (ratio of 5:1) for different times. Mo and MDM were labeled with BODIPY phalloidin, and the binding of AL and NL was quantified by fluorescence microscopy. The results are expressed as the percentage of Mo (E) and MDM (F) that have bound at least one AL or NL. More than 100 cells were examined by experimental condition. The results represent the mean \pm SEM of 5 experiments.

doi:10.1371/journal.ppat.1000066.g002

(qPCR). Mo that had bound AL allowed *C. burnetii* replication after 9 days of culture ($29,000 \pm 3,000$ vs. $12,600 \pm 2,000$ bacterial DNA copies in control Mo, $p < 0.001$; Figure 3A). In MDM that had bound AL, *C. burnetii* replication was detectable after 3 days and was significantly ($p < 0.05$) higher at day 9 ($45,000 \pm 2,000$ vs. $24,280 \pm 2,200$ bacterial DNA copies in control MDM, Figure 3B). The effect of AL was independent of the apoptosis-inducer agent since the replication of *C. burnetii* was increased in Mo and MDM that have bound apoptotic cells induced by either corticoids or staurosporine (data not shown). In contrast to AL binding, the

binding of NL to Mo (Figure 3A) and MDM (Figure 3B) induced *C. burnetii* killing. After 9 days of culture, the bacterial load was significantly ($p < 0.05$) decreased by 66% in Mo (Figure 3A) and by 50% in MDM (Figure 3B), as compared with control cells. Bacterial infection was also determined by immunofluorescence. The percentage of Mo (Figure 3C) and MDM (Figure 3D) that contained more than 5 bacteria increased after the binding of AL. It reached about 25% after 9 days of culture, while this percentage did not exceed 15% in control Mo and MDM ($p < 0.001$). In contrast, the number of Mo and MDM containing more than 5

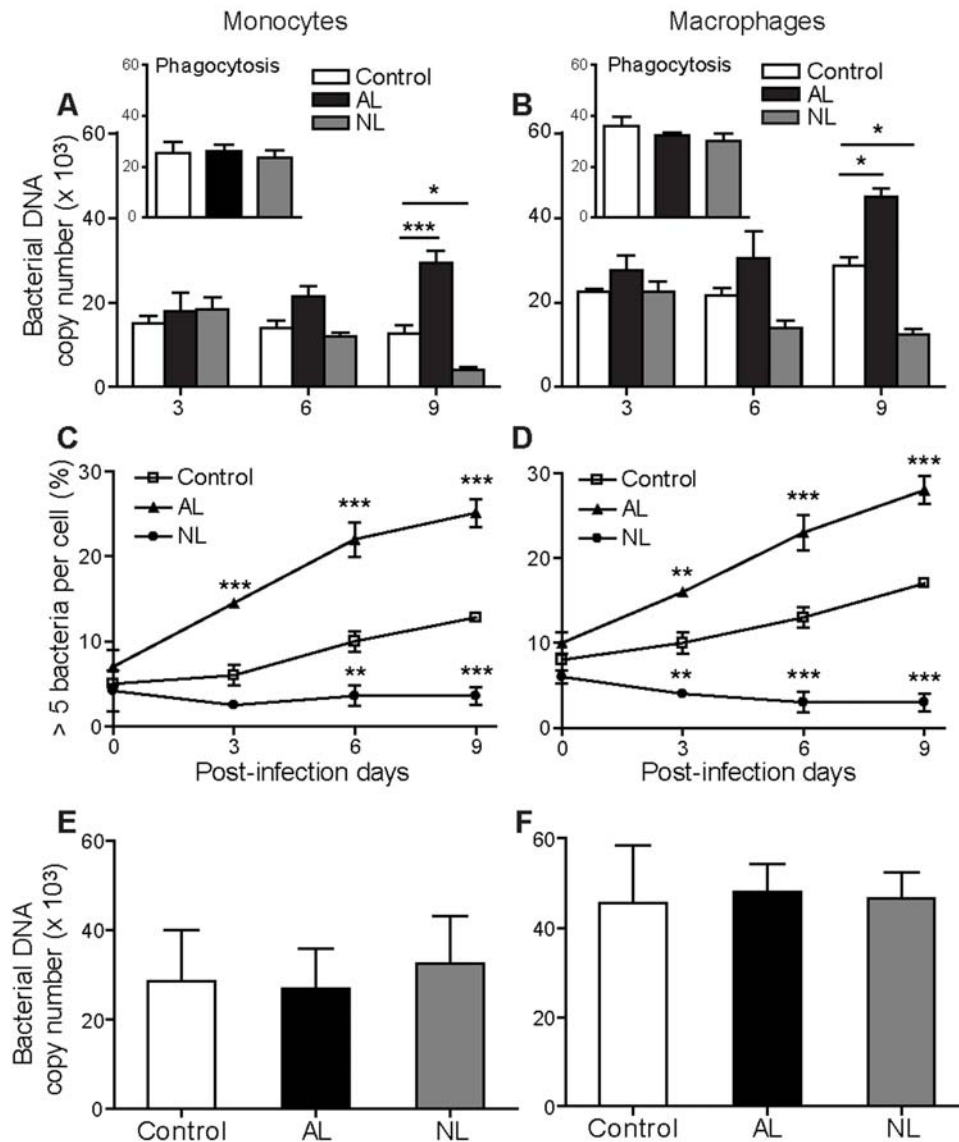


Figure 3. Effect of AL binding on the intracellular survival of *C. burnetii*. A–D, Mo (A, C) and MDM (B, D) were incubated with AL or NL for 2 h, infected with *C. burnetii* for 4 h (insets) and cultured for 9 days. The number of bacterial DNA copies was determined by qPCR in Mo (A) and MDM (B). The percentages of Mo (C) and MDM (D) that bound more than 5 bacteria were determined by indirect immunofluorescence. The results represent the mean \pm SEM of 5 experiments. E and F, Mo (E) and MDM (F) were incubated with AL and NL in separate chambers for 2 h, then infected with *C. burnetii* for 4 h, and cultured for 9 days. The number of bacterial DNA copies was determined by qPCR at day 9. The results represent the mean \pm SEM of 3 experiments. * $p < 0.05$, ** $p < 0.01$ and *** $p < 0.001$. doi:10.1371/journal.ppat.1000066.g003

bacteria was significantly ($p < 0.001$) lower after NL binding (Figure 3C and D). Taken together, these results showed that AL binding stimulated *C. burnetii* replication in Mo and MDM, while the NL binding led to *C. burnetii* killing. Finally, the effect of AL and NL on *C. burnetii* replication was cell-contact dependent since the culture of Mo (Figure 3E) and MDM (Figure 3F) with AL and NL in separate chambers had no effect on *C. burnetii* replication.

In macrophages, *C. burnetii* survives in a late phagosome that fails to fuse with lysosomes [17]. The effect of AL binding on the intracellular traffic of *C. burnetii* in MDM was studied by determining the colocalization of *C. burnetii* with Lamp-1 (Lysosomal associated membrane protein-1), a marker of the late endosomes-early lysosomes, and the lysosomal protease cathepsin D. In control MDM, *C. burnetii* resided in a late phagosome unable to fuse with lysosomes (Figure 4A). Indeed, $78 \pm 6\%$ of *C. burnetii*

phagosomes were Lamp-1⁺ and cathepsin D⁻ while only $22 \pm 8\%$ of phagosomes expressed both Lamp-1 and cathepsin D (Figure 4D). The binding of AL (Figure 4B) and NL (Figure 4C) to MDM increased the maturation of the *C. burnetii* phagosome toward a mature phagolysosome: about 60% of *C. burnetii* phagosomes were Lamp-1⁺ and cathepsin D⁺ after binding of AL or NL (Figure 4D). Thus, AL and NL binding to MDM stimulated the maturation of *C. burnetii* phagosomes in the early phase of infection.

Effect of AL binding on the polarization of *C. burnetii*-infected Mo and MDM

We hypothesized that AL binding may orient Mo and MDM toward a M2 program that favors *C. burnetii* replication. Transcriptional patterns of AL-Mo and AL-MDM were compared

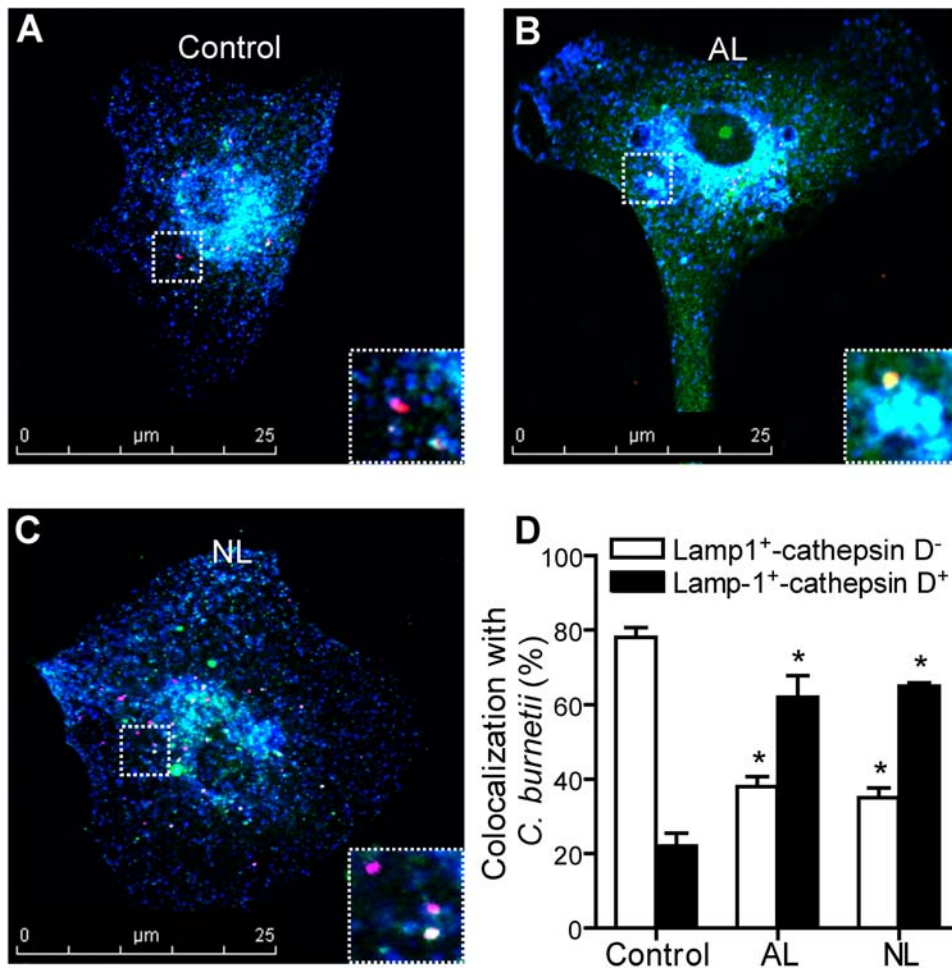


Figure 4. Effect of AL binding on the maturation of *C. burnetii*-phagosomes. MDM (A), AL-MDM (B) or NL-MDM (C) were stimulated with *C. burnetii* for 4 h, washed and then cultured for 24 h. Cells were labeled with anti-*C. burnetii* (Alexa 546), anti-Lamp-1 (Alexa 488) and anti-cathepsin D (Alexa 647) Abs and analyzed under a confocal microscope. A–C, Representative micrographs are shown with expanded images (white rectangle). D, Percentage of *C. burnetii* phagosomes that colocalized with Lamp-1 and cathepsin D. The results represent the mean \pm SEM of 4 independent experiments. * $p < 0.01$.

doi:10.1371/journal.ppat.1000066.g004

by clustering algorithm analysis (Figure 5A). Mo and MDM stimulated with *C. burnetii* exhibited distinct transcriptional programs that combine M1 and M2 features. The expression of CCL18, CCL24 and Fc ϵ -R2, associated with the M2 profile, and CD1B, CD1C and CD1D were up-regulated in both cell types. In Mo, *C. burnetii* up-regulated the expression of CCL20, which is associated with M2 polarization; CCR7 and TNF, which are associated with M1 polarization; and CD1A and Fc α -R. It only down-regulated the expression of IL-20. In *C. burnetii*-infected MDM, the expression of CCL16 and IL-1ra, which are associated with M2 polarization, and that of CXCL8, CXCL11 and IL-6, which are associated with M1 polarization, were up-regulated. The expression of the two M1 cytokines IFN- γ and TNF were down-regulated. AL binding directed *C. burnetii*-infected Mo and MDM toward a M2 program. In Mo, AL binding up-regulated the expression of CCL16, CD14, IL-10, IL-1ra, which are associated with M2 polarization, IL-6, IL-13 and the three members of the IL-10 family, IL-19, IL-20 and IL-24. AL binding also down-regulated numerous genes involved in M1 polarization, such as CCR7, IL-12p40, IL-1 β , TNF and iNOS. In MDM, AL binding up-regulated the expression of IL-10, IL-1ra and TGF- β 1, which are associated with M2 polarization; and CXCL10 and IL-

6, which are associated with M1 polarization. The expression of the M1 markers CXCL8, CCR7, IL-12p40, IL-1 β and TNF were down-regulated. In contrast to AL binding, NL binding stimulated a typical M1 profile in *C. burnetii*-infected Mo and MDM. Indeed, NL binding up-regulated the expression of the M1 molecules CCL5, CXCL8, CXCL11, CCR7, CD80, IFN- γ , TNF, IL-12p40, IL-1 β and iNOS in both Mo and MDM (Figure 5A).

Functional tests confirmed the transcriptional studies. After AL binding, Mo exhibited a M2 program characterized by high levels of IL-10 and IL-6, decreased TNF release (Figure 5B) and increased expression of CD14 ($p < 0.05$, Figure 5D). As found for transcriptional responses, the response of MDM was characterized by M2 features that were partly different from those of Mo. Indeed, AL-MDM released high levels of TGF- β 1 (Figure 5C) and the percentage of MDM that expressed MR was significantly ($p < 0.001$) increased (Figure 5E). The effect of AL binding was specific since NL binding induced a M1 program in both Mo and MDM stimulated with *C. burnetii*. Indeed, the release of TNF by Mo and MDM was increased whereas those of IL-6, TGF- β 1 and IL-10 were inhibited (Figure 5B and C). In addition, the expression of CD14 in Mo ($p < 0.001$, Figure 5D) and that of MR in MDM ($p < 0.01$, Figure 5E) were significantly decreased.

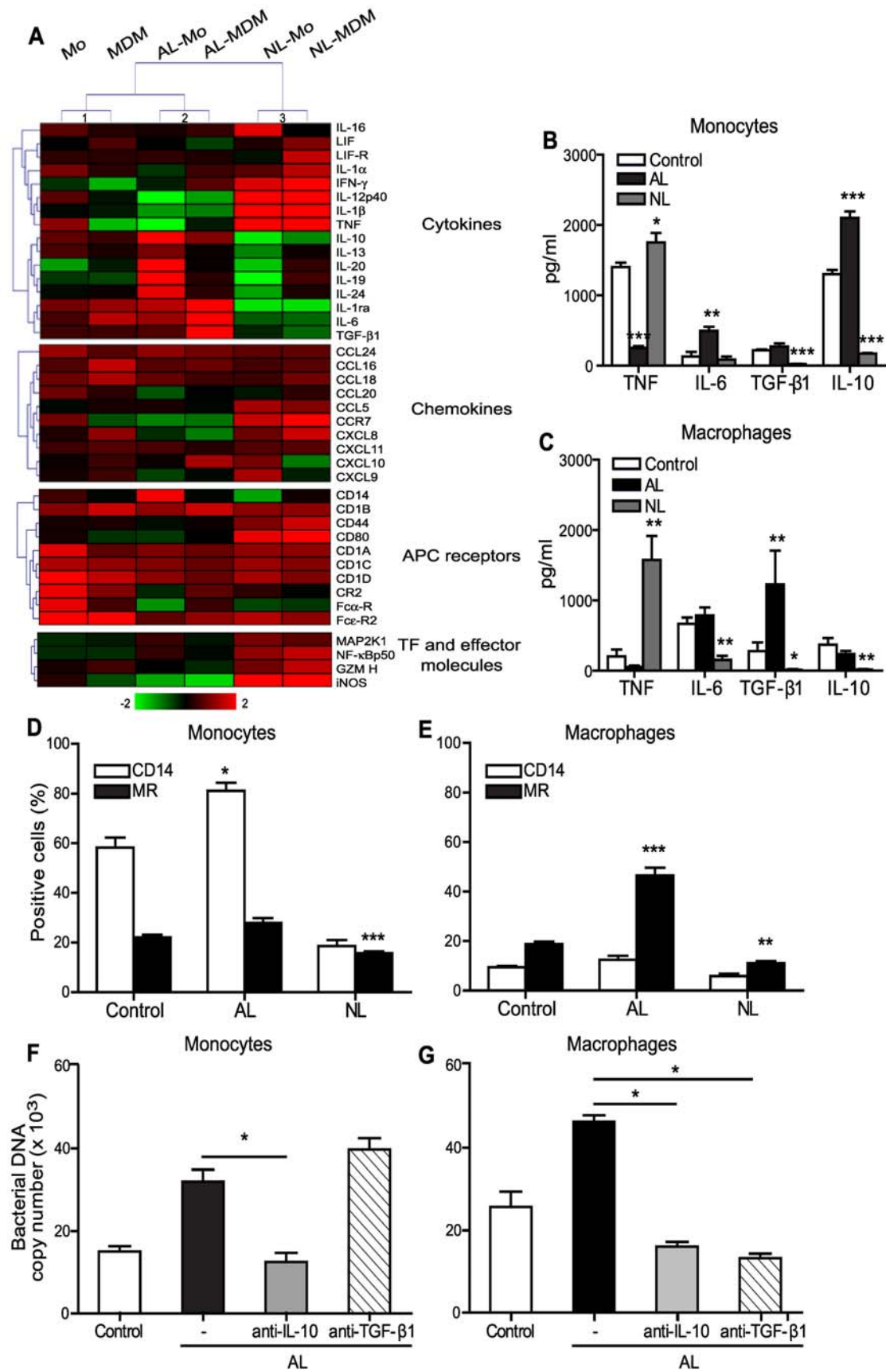


Figure 5. Polarization of *C. burnetii*-stimulated Mo and MDM after AL uptake. A, Transcriptional responses of *C. burnetii*-stimulated Mo and MDM that had bound AL or NL were analyzed by DNA microarrays. Modulated genes (fold-change ≥ 2) were compared by hierarchical clustering analysis. APC, antigen presenting cells and TF, transcription factors. B and C, Cytokine release by *C. burnetii*-stimulated Mo (B) and MDM (C) after AL or NL uptake. The results are expressed in pg/ml and represent the mean \pm SEM of 5 experiments. D and E, Membrane expression of CD14 and MR on *C. burnetii*-stimulated Mo (D) and MDM (E) after AL or NL binding. The results are expressed as the percentages of positive cells and represent the mean \pm SEM of 5 experiments. F and G, Mo and MDM were incubated with AL for 2 h and then infected with *C. burnetii* for 4 h. Cells were then cultured for 9 days in the presence of 10 μ g/ml of monoclonal anti-IL-10 or anti-TGF- β 1 Abs. The number of bacterial DNA copies was determined by qPCR. The results represent the mean \pm SEM of 3 experiments. * $p < 0.05$, ** $p < 0.01$ and *** $p < 0.001$. doi:10.1371/journal.ppat.1000066.g005

Finally, we showed that IL-10 was critically involved in the replication of *C. burnetii* since adding blocking anti-IL-10 antibodies (Abs) to AL-Mo (Figure 5F) and AL-MDM (Figure 5G) prevented bacterial replication. Anti-TGF- β 1 blocking Abs prevented the replication of *C. burnetii* only in AL-MDM and had no effect in AL-Mo (Figure 5F and G). Taken together, these results showed that AL binding stimulated a clear-cut M2 profile in Mo and MDM, in which IL-10 appears critical in both Mo and MDM and TGF- β 1 in MDM.

Effect of IFN- γ on *C. burnetii* replication and macrophage polarization

As IFN- γ stimulates *C. burnetii* killing in Mo and MDM [24], we wondered if it may correct the permissive effect of AL binding on *C. burnetii* replication. IFN- γ inhibited *C. burnetii* replication in AL-Mo (Figure 6A) and AL-MDM (Figure 6B). After 9 days of culture, the bacterial DNA copy number decreased from $31,100 \pm 1,330$ in AL-Mo to $8,300 \pm 450$ in IFN- γ -treated AL-Mo ($p < 0.001$). In AL-MDM, the bacterial DNA copy number decreased from $47,340 \pm 2000$ to $18,400 \pm 3,800$ in IFN- γ -treated cells ($p < 0.05$). The number of bacterial DNA copies was similar to that found in Mo and MDM treated with IFN- γ . The percentage of cells that contained more than 5 bacteria was also significantly ($p < 0.05$) lower in IFN- γ -treated AL-Mo and AL-MDM (Figure S2), demonstrating that IFN- γ completely reverted the effect of AL binding on *C. burnetii* replication. In addition, IFN- γ increased the maturation of *C. burnetii* phagosomes toward phagolysosomes independently of AL binding: more than 90% of *C. burnetii* phagosomes were Lamp-1 and cathepsin D positive after IFN- γ treatment (Figure 6C–E). Finally, IFN- γ reverted the response of AL-Mo and AL-MDM toward a M1 profile. First, it caused up-regulation of CXCL8, TNF and iNOS genes and down-regulation of IL-6 and IL-10 genes in AL-Mo. It also down-regulated the expression of TGF- β 1 in AL-MDM (Figure 6F). Second, the IFN- γ treatment of AL-Mo and AL-MDM induced the release of high levels of TNF and inhibited the release of IL-6, IL-10 and TGF- β 1 (Figure 6G). These results showed that IFN- γ prevented the effect of AL binding on *C. burnetii* replication and polarized AL-Mo and AL-MDM toward a M1 profile.

Discussion

Patients with cardiac valve lesions have the highest risk to develop IE [2], although the role of valvulopathy in the establishment of IE is not clearly elucidated. We showed here, for the first time, that patients with valvulopathy exhibited increased levels of circulating apoptotic leukocytes, suggesting a link between valvulopathy and leukocyte apoptosis. We have previously demonstrated that Q fever endocarditis is associated with immune impairment [25,26]. The immune impairment may be due to lymphopenia induced by lymphocyte cell death but lymphopenia was not reported in Q fever endocarditis [14]. We hypothesized that the binding of apoptotic leukocytes to Mo and macrophages may be responsible for the immune impairment observed in Q fever endocarditis. To test this

hypothesis, we have established an *in vitro* model to study the effect of apoptotic cells on *C. burnetii* replication.

Binding of AL to Mo and macrophages induced the formation of large membrane ruffles with local F-actin redistribution. This result is in accordance with previous reports that showed that adhesion of apoptotic cells to specific membrane receptors leads to the formation of large membrane ruffles and cytoskeleton reorganization [27,28]. We showed for the first time that NL binding induced cytoskeletal reorganization characterized by the formation of filopodia with F-actin concentration at their basis. The differences in cytoskeletal changes induced by AL and NL in Mo and MDM were not due to differences in binding levels: about 80% of Mo and MDM ingested AL and NL after 2 hours. They may result from the engagement by AL and NL of specific receptors that further modulate cytoskeleton reorganization in different ways [18,29].

The binding of AL increased *C. burnetii* replication in Mo and MDM as do IL-10, the only cytokine able to stimulate *C. burnetii* replication [30]. Our results emphasized recent studies on the impact of the binding of apoptotic cells to phagocytes on survival of intracellular pathogens. The binding of apoptotic cells to murine macrophages increases the replication of the avirulent form of *C. burnetii* [31] and the growth of *Trypanosoma cruzi* [32] and *Leishmania major* [33]. In addition, the replication of *C. burnetii* induced by AL is dependent on AL contact with Mo and MDM. It has been previously demonstrated that the contact between monocytes and apoptotic cells is required for inducing the immunosuppressive response of monocytes [34]. Finally, the receptors engaged by AL binding are likely critical for *C. burnetii* replication. Indeed, when AL were opsonized (Protocol S1) with specific Abs to engage the Fc-receptor (FcR) pathway, the replication of *C. burnetii* was prevented (Figure S3). These results are supported by the fact that apoptotic cells opsonized with antibodies, particularly IgG, are recognized by macrophage FcR and stimulate a pro-inflammatory response [35]. This also suggests that the entry pathway orients the intracellular fate of *C. burnetii*.

Interestingly, the binding of AL or NL to macrophages increased the maturation of *C. burnetii* phagosomes. It has been recently shown that the uptake of apoptotic cells by macrophages or fibroblasts results in a rapid maturation of phagosomes by stimulating Rho GTPases [36]. It is tempting to speculate that the maturation of *C. burnetii* phagosomes observed after NL binding results also in the activation of Rho GTPases in Mo and MDM. However, the increased maturation of *C. burnetii* phagosomes, which occurs early during the *C. burnetii* infection, did not seem to govern the intracellular fate of bacteria in the later stages of infection.

AL binding by *C. burnetii*-infected Mo and MDM reprogrammed them toward a M2 profile, but the properties of the M2 programs were different in Mo and MDM. In AL-Mo, the expression of genes encoding four members of the IL-10 family, namely IL-10, IL-19, IL-20 and IL-24, were up-regulated. The four genes are expressed within a highly conserved cluster [37]. IL-10 is highly secreted by macrophages following ingestion of apoptotic cells [38]. IL-10 is also critically implicated in the persistence of

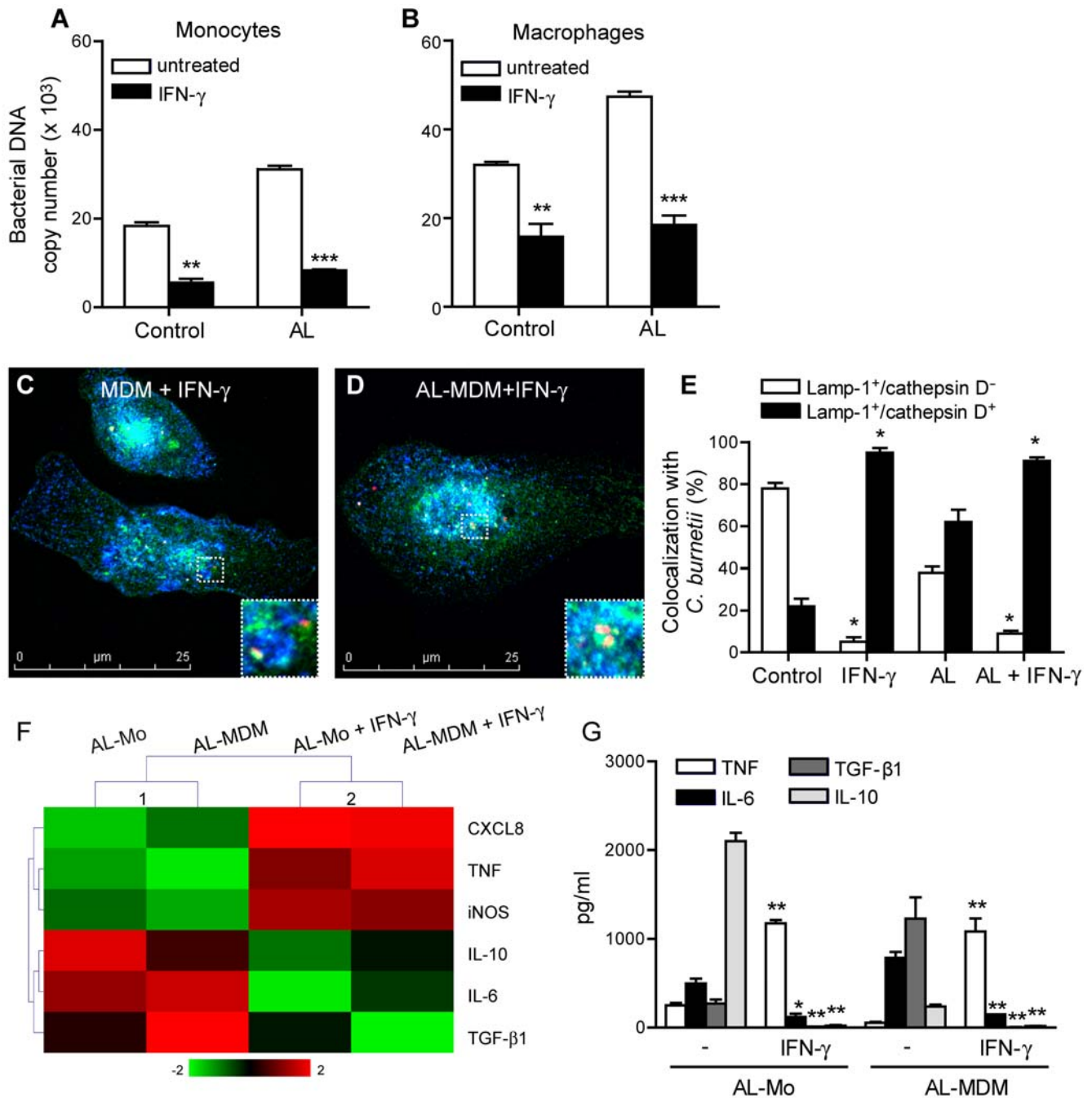


Figure 6. Effect of IFN- γ on AL-Mo and AL-MDM responses. Mo and MDM that had or not ingested AL were infected with *C. burnetii* for 4 h in the presence of 1000 U/ml of IFN- γ . A and B, After washing, Mo and AL-Mo (A) or MDM and AL-MDM (B) were cultured for 9 days in the presence of IFN- γ . *C. burnetii* replication was determined by qPCR. The results represent the mean \pm SEM of 3 experiments. C–E, After washing, MDM and AL-MDM were cultured for 24 h in the presence of IFN- γ . Cells were labeled with anti-*C. burnetii* (Alexa 546), anti-Lamp-1 (Alexa 488) and anti-cathepsin D (Alexa 647) Abs and analyzed under a confocal microscope. Representative micrographs of IFN- γ -treated MDM (C) and AL-MDM (D) are shown with expanded images (white rectangle). In E, the results are expressed as the percentages of *C. burnetii* phagosomes that colocalised with Lamp-1 and/or cathepsin D. F, The transcriptional response of AL-Mo and AL-MDM stimulated with *C. burnetii* for 4 h in the presence or the absence of IFN- γ was analyzed by qRT-PCR. The results are expressed as the Log₂ fold change and analyzed by hierarchical clustering. G, AL-Mo and AL-MDM were stimulated with heat-killed *C. burnetii* for 24 h in the presence or the absence of IFN- γ . The cytokine release was determined by immunoassays and expressed in pg/ml. The results represent the mean \pm SEM of 3 experiments. * $p < 0.05$, ** $p < 0.01$ and *** $p < 0.001$. doi:10.1371/journal.ppat.1000066.g006

microorganisms and the chronic evolution of Q fever [39]. IL-19 and IL-20 down-regulate IFN- γ expression and up-regulate that of IL-4 and IL-13 in T cells, supporting a Th2 polarization [40]. In Mo, AL binding up-regulated also the expression of IL-1ra, which

is increased in patients with Q fever [41]. In MDM, AL binding up-regulated the expression of TGF- β 1, which is known to interfere with the activities of IFN- γ , iNOS and superoxide anion [42–44], alter the expression of co-stimulatory molecules [45],

inhibit Th1/Th2 differentiation [46] and favor the expansion of regulatory T cells [47]. Interestingly, patients with acute Q fever and valvulopathy or Q fever endocarditis exhibit higher numbers of regulatory T cells as compared to patients with acute Q fever and healthy persons (our unpublished data). We also found that IL-6 was up-regulated in both AL-Mo and AL-MDM. IL-6 is largely considered as an enhancer of the inflammatory response. However, IL-6 can also act as a modulator of inflammatory responses since it shifts the T cell response toward a Th2 response by inducing B cell maturation [48]. Recently, it has been reported that IL-6 and TGF- β 1 act together in inducing IL-10 production in T cells [49]. We can suppose that, in Q fever, IL-6 may contribute to the defective control of *C. burnetii* infection by macrophages. Finally, the replication of *C. burnetii* stimulated by AL binding was strongly associated with the production of M2 cytokines since IL-10 and TGF- β 1 neutralization abolished bacterial replication. These results suggest a direct role of IL-10 and TGF- β 1 in the signaling pathway leading to *C. burnetii* replication.

In contrast to AL binding, NL binding induced *C. burnetii* killing and a M1 transcriptional program in Mo and MDM. These results confirmed previous studies on the bactericidal response of Mo and MDM against *C. burnetii* induced by inflammatory cytokines, such as IFN- γ [24]. In addition, the expression of genes associated with a M2 program was down-regulated: peculiarly, the gene encoding IL-10 was inhibited in NL-Mo while the gene encoding TGF- β 1 was inhibited in NL-MDM. Our results are consistent with other reports. The binding of necrotic cells induces the release of inflammatory cytokines by MDM [50]. It also induces the expression of major histocompatibility complex class II molecules by antigen-presenting cells and increases their ability to activate T cells [51].

Finally, IFN- γ inhibited the effect of AL binding on the *C. burnetii* replication in Mo and MDM. It induced *C. burnetii* killing and complete maturation of *C. burnetii* phagosomes. In contrast to LPS that is unable to inhibit the anti-inflammatory response of peripheral blood mononuclear cells (PBMCs) and Mo after binding of apoptotic cells [19,34], IFN- γ reverted the M2 program induced by AL. It is likely that *C. burnetii* infection amplifies the inflammatory signal induced by IFN- γ to engage Mo and MDM toward a M1 profile. We can also suppose that the engagement of a broad number of receptors by *C. burnetii*, such as TLR4 [52], TLR2 [53] and the α v β 3 integrin [54], in the presence of IFN- γ counter-balances the anti-inflammatory signals delivered by AL to phagocytic cells.

In conclusion, we showed that valvulopathy increased the rate of circulating apoptotic leukocytes and we provided a model in which apoptotic cells play a key role in the establishment of Q fever endocarditis (Figure 7). The binding of apoptotic cells increased *C. burnetii* replication by subverting phagocyte responses; Mo and MDM, polarized toward M2 profiles, stimulate type 2 responses that are non-protective against most pathogens. If the systemic apoptosis of leukocytes occurs in an inflammatory context, such as that found in the presence of IFN- γ , the effect of AL binding is inhibited; Mo and MDM, polarized toward a M1 program, are able to kill *C. burnetii* as do patients with acute Q fever without valvulopathy. Our results give new comprehensive insights into the pathological processes resulting from valvulopathy that are associated with the high risk to develop rare and atypical IE.

Materials and Methods

Patients

Informed and written consent was obtained from each subject and the study was approved by the Ethics Committee of the

Université de la Méditerranée. Nine patients with valvulopathy (5 men and 4 women, mean age of 69.5 years), 10 with acute Q fever (3 men and 7 women, mean age of 46.3 years), 11 with acute Q fever and valvulopathy (6 men and 5 women, mean age of 51.3 years) and 11 with Q fever endocarditis (7 men and 4 women, mean age of 47.6) were included. Ten healthy persons (6 men and 4 women, mean age of 35.0 years) were included as controls. The diagnosis of acute and chronic Q fever was based on epidemiological and clinical features, as previously described [55].

Circulating apoptosis markers

Plasma levels of nucleosomes were measured using the ELISA cell death detection plus kit from Roche Diagnostics. This assay is based on a quantitative sandwich enzyme immunoassay that recognizes DNA and histones [56]. The specific enrichment factor in nucleosomes, expressed in arbitrary units, was calculated as previously described [57].

Caspase activity of leukocytes was measured with the Apoptosis Detection Polycaspase Assay Kit (Immunochemistry Technologies), as previously described [57]. Briefly, 100 μ l of EDTA-collected blood were incubated with 5 μ l of 30 \times FLICA solution for 1 h and then with 20 μ l of CD3-PE or CD14-APC for 15 min. After washing, leukocytes were fixed and analyzed by flow cytometry (EPICS XL, Coulter Beckman). The percentage of CD3⁺ or CD14⁺ leukocytes with active caspases was determined using the Expo32 ADC and the WinMDI 2.8 software.

Bacteria

C. burnetii organisms (Nine Mile strain) were cultured as previously described [54]. Dilacerated spleens of BALB/c mice infected with 10⁸ *C. burnetii* organisms for 7 days were added to L929 cells. Infected cells were sonicated and centrifuged at 300 \times g for 10 min. Supernatants were collected and centrifuged at 10,000 \times g for 10 min. Bacteria were then washed and stored at -80°C. The concentration of organisms was determined by Gimenez staining and the bacterial viability was assessed using the LIVE/DEAD BacLight bacterial viability kit (Molecular Probes).

Cell isolation and culture

PBMCs were isolated from leukopacks (Etablissement Français du Sang, Marseille, France) by Ficoll gradient (MSL, Eurobio) and suspended in RPMI 1640 containing 20 mM HEPES, 10% fetal calf serum (FCS), 2 mM L-glutamine, 100 U/ml penicillin and 100 μ g/ml streptomycin (Invitrogen). PBMCs were incubated in flat-bottom 24-well plates (Nunc) for 60 min at 37°C. After washing, adherent cells were designated as Mo (90% of cells expressed CD14) and MDM were obtained by a 7-day culture, as recently described [58]. Non-adherent cells were designated as lymphocytes (90% of them expressed CD3). Lymphocyte apoptosis, induced by incubation with dexamethasone (Merck) for 24 h [59], and necrosis, induced by heat shock, were determined by flow cytometry using the annexin V/Propidium Iodide (PI) kit (Roche) (Figure S1). Mo and MDM were incubated with AL or NL (ratio of 1:5) for different periods, washed to remove unbound AL or NL, and infected with *C. burnetii*. In some experiments, Mo and MDM were separated from AL or NL using culture inserts (0.4- μ m pore size; Transwell, Costar) in 24-well plates before *C. burnetii* infection.

C. burnetii infection of Mo and MDM

Mo and MDM were incubated with *C. burnetii* (bacterium-to-cell ratio of 200:1) for 4 h. After washing to remove free bacteria (time designated as day 0), infected cells were cultured for 12 days. In

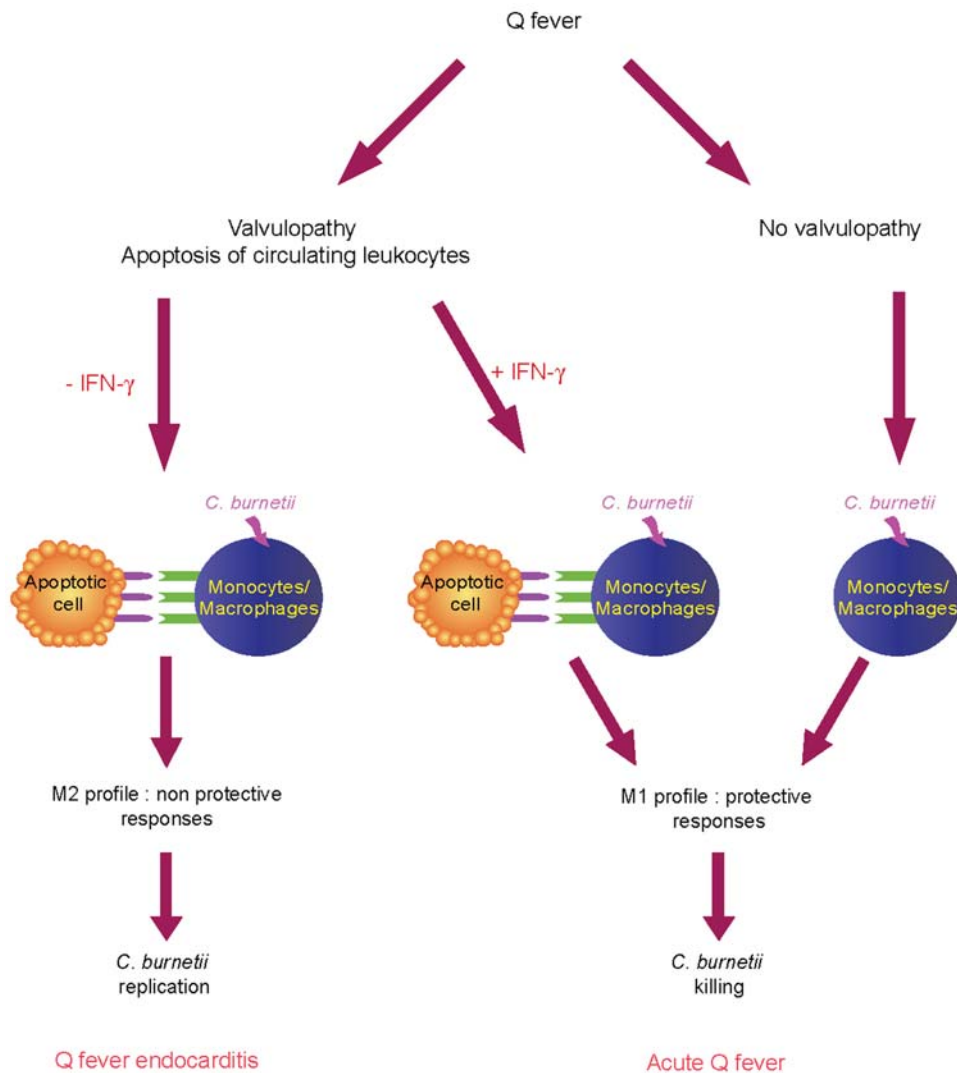


Figure 7. Leukocyte apoptosis and Q fever evolution. Valvulopathy is associated with increased apoptosis of circulating leukocytes. In the model of Q fever endocarditis, the uptake of apoptotic cells by Mo and MDM increases bacterial replication through the polarization of Mo and MDM toward M2 profiles that are non-protective against most pathogens. In patients without valvulopathy or in immunocompetent patients that produce IFN- γ , Mo and MDM are polarized toward a M1 program and are able to kill *C. burnetii*. doi:10.1371/journal.ppat.1000066.g007

some experiments, recombinant human IFN- γ (1000 U/ml, Peptrotech Inc.), monoclonal anti-IL-10 (10 μ g/ml, R&D Systems) or anti-TGF- β 1 (10 μ g/ml, R&D Systems) Abs were added every 3 days. Infection was quantified by immunofluorescence [52] and qPCR. DNA was extracted with the QIAamp Blood Mini Kit (Qiagen) and stored in a volume of 100 μ l at -20° C. qPCR was performed using 5 μ l of DNA extract and the LightCycler FastStart DNA SYBR green system (Roche), as previously described [60]. Primers (Table S1) amplified a 75-bp fragment of the *C. burnetii com1* gene (GenBank accession no. AF318146).

C. burnetii intracellular trafficking

MDM were infected with *C. burnetii* for 4 h (bacterium-to-cell ratio of 200:1), washed and cultured for 24 h. Cells were fixed in 3% paraformaldehyde, permeabilized with 0.1% Triton X-100 and immunofluorescence labeling was performed according to standard procedures [61]. Briefly, MDM were incubated with human anti-*C. burnetii* (1:4,000 dilution), mouse anti-Lamp-1 (1:1,000 dilution, DHSB, Developmental Studies Hybridoma

Bank) and rabbit anti-cathepsin D (1:1,000 dilution, a gift from S. Kornfeld, Washington University School of Medicine, St. Louis, Missouri) Abs for 30 min. Bacteria were revealed by Alexa 546-conjugated F(ab')₂ anti-human IgG Abs, Lamp-1 by Alexa 488-conjugated anti-mouse IgG Abs and cathepsin D by Alexa 647-conjugated anti-rabbit IgG Abs. All secondary Abs were used at a 1:500 dilution. The colocalization of bacteria and intracellular markers was examined by laser scanning microscopy using a confocal microscope (Leica TCS SP2) with a 63 \times /1.32-0.6 oil CS lens and an electronic Zoom 3 \times . Optical sections of fluorescent images were collected at 0.25- μ m intervals using the Leica Confocal software and processed using the Adobe Photoshop V5.5 software. At least 65 MDM were examined for each experimental condition and the results are expressed as the percentage of bacteria that colocalized with fluorescent markers.

Transcriptional profile of Mo and MDM

Mo and MDM were stimulated with *C. burnetii* for 4 h. Total RNA was purified using the RNeasy Mini Kit (Qiagen), according

to the manufacturer's protocol. DNase treatment was performed with the RNase-free DNase set (Qiagen). The transcriptional pattern of cells was studied using a cDNA chip containing 440 arrayed sequences (Oligo GEArray Human Hematology/Immunology, SuperArray). Ten μg of RNA were transcribed into biotin-labeled cDNA by the MMLV reverse transcriptase (RT). Membranes were then hybridized with biotin-labeled cDNA and incubated with streptavidin-conjugated alkaline phosphatase. Chemiluminescence was visualised by autoradiography. Datasets were analyzed with the GEArray Expression Analysis Suite software (SuperArray) and the TIGR's Multiexperiment Viewer. Data were submitted to the ArrayExpress database (MIAME Accession number E-MEXP-1289). For qRT-PCR studies, reverse transcription of RNA was performed with the MMLV-RT kit (Invitrogen), according to the manufacturer's protocol. The primers (Supplemental data, Table I) were designed using the primer3 tool (http://frodo.wi.mit.edu/cgi-bin/primer3/primer3_www.cgi). RT was omitted in negative controls. The fold change in target gene cDNA relative to the β -actin endogenous control was determined as follows: fold change = $2^{-\Delta\Delta\text{Ct}}$, where $\Delta\text{Ct} = (\text{Ct}_{\text{Target}} - \text{Ct}_{\text{Actin}})_{\text{test condition}} - (\text{Ct}_{\text{Target}} - \text{Ct}_{\text{Actin}})_{\text{reference condition}}$. Ct values were defined as the number of cycles for which the fluorescence signals were detected [62].

Immunoassays

Mo and MDM were incubated with heat-killed (100°C for 30 min) *C. burnetii* organisms (bacterium-to-cell ratio of 10:1) for 24 h. Supernatants were stored at -80°C before immunoassays. IL-10, TGF- β 1 and TNF assays were purchased from R&D Systems. IL-6 assay was purchased from Beckman Coulter. The intra- and interspecific coefficients of variation ranged from 5% to 10%.

Flow cytometry

Mo and MDM (5×10^5 cells per well) were incubated with AL and NL for 2 h, washed and then stimulated with *C. burnetii* (bacterium to cell ratio of 10:1) for 24 h. After washing, Mo and MDM were scrapped and washed once with ice-cold PBS. Mo and MDM were then incubated with 10 μl of CD14-PE (Beckman Coulter) and MR-FITC (BioLegend, San Diego, California, USA) Abs for 30 min at 4°C. Cells were washed three times in ice-cold PBS and resuspended in PBS containing 10% FCS and 1% sodium azide (Sigma-Aldrich). Cells were then stored at 4°C in the dark and analyzed by flow cytometry (EPICS XL, Beckman Coulter). Ten thousand events were acquired for each sample. The percentage of positive cells was determined using the Expo32 ADC and the WinMDI 2.8 software.

References

- Durack DT (1995) Prevention of infective endocarditis. *N Engl J Med* 332: 38–44.
- Wilson W, Taubert KA, Gewitz M, Lockhart PB, Baddour LM, et al. (2007) Prevention of infective endocarditis: guidelines from the American Heart Association: a guideline from the American Heart Association Rheumatic Fever, Endocarditis and Kawasaki Disease Committee, Council on Cardiovascular Disease in the Young, and the Council on Clinical Cardiology, Council on Cardiovascular Surgery and Anesthesia, and the Quality of Care and Outcomes Research Interdisciplinary Working Group. *J Am Dent Assoc* 138: 739–745, 747–760.
- Durack DT, Beeson PB (1972) Experimental bacterial endocarditis. I. Colonization of a sterile vegetation. *Br J Exp Pathol* 53: 44–49.
- Hamill RJ (1987) Role of fibronectin in infective endocarditis. *Rev Infect Dis* 9 Suppl 4: S360–371.
- Sinha B, Francois P, Que YA, Hussain M, Heilmann C, et al. (2000) Heterologously expressed *Staphylococcus aureus* fibronectin-binding proteins are sufficient for invasion of host cells. *Infect Immun* 68: 6871–6878.

Statistical analysis

Results are expressed as medians or means \pm SEM and compared with the non-parametric Mann-Whitney *U* test. Differences were considered significant when $p < 0.05$.

Supporting Information

Table S1 Sequences of primers used in qPCR experiments
Found at: doi:10.1371/journal.ppat.1000066.s001 (0.04 MB DOC)

Figure S1 Induction of lymphocyte apoptosis and necrosis. A and B, Lymphocytes were incubated with different concentrations of dexamethasone for 24 h, labelled with annexin V-FITC and PI (A) or poly-caspases-FITC (B) and analysed by flow cytometry. C, Lymphocytes were heated at 56°C or 95°C for 15 min, labelled with annexin V-FITC and PI and analysed by flow cytometry. The results represent the mean \pm SEM of 5 independent experiments.

Found at: doi:10.1371/journal.ppat.1000066.s002 (3.09 MB TIF)

Figure S2 Effect of IFN-gamma on the replication of *C. burnetii* induced by AL uptake. Mo and AL-Mo (A) and MDM and AL-MDM (B) were infected with *C. burnetii* for 4 h and then cultured for 9 days in the presence of IFN-gamma. *C. burnetii* replication was determined by immunofluorescence. The results represent the mean \pm SEM of 3 independent experiments. * $p < 0.05$

Found at: doi:10.1371/journal.ppat.1000066.s003 (1.44 MB TIF)

Figure S3 Effect of AL opsonization on *C. burnetii* replication. AL were opsonized with mouse polyclonal Abs for 30 min before incubation with Mo (A) and MDM (B) for 2 h. Cells were then washed and infected with *C. burnetii* for 4 h. Mo and MDM were cultured for 9 days. Every 3 days, cells were lysed, and bacterial infection was determined by qPCR. The results represent the mean \pm SEM of 3 independent experiments. * $p < 0.05$ and ** $p < 0.01$.

Found at: doi:10.1371/journal.ppat.1000066.s004 (2.42 MB TIF)

Protocol S1 Mouse polyclonal Abs against human AL
Found at: doi:10.1371/journal.ppat.1000066.s005 (0.03 MB DOC)

Acknowledgments

We are grateful to M. Zerial and the Light Microscopy Facility (LMF) team (Dresden, Germany) for their assistance.

Author Contributions

Conceived and designed the experiments: MB JM. Performed the experiments: MB EG. Analyzed the data: MB EG JM. Contributed reagents/materials/analysis tools: MB EG CC DR JM. Wrote the paper: MB CC DR JM.

11. Shive MS, Brodbeck WG, Colton E, Anderson JM (2002) Shear stress and material surface effects on adherent human monocyte apoptosis. *J Biomed Mater Res* 60: 148–158.
12. Houpiikian P, Raoult D (2005) Blood culture-negative endocarditis in a reference center: etiologic diagnosis of 348 cases. *Medicine (Baltimore)* 84: 162–173.
13. Raoult D, Marrie T, Mege JL (2005) Natural history and pathophysiology of Q fever. *Lancet Infect Dis* 5: 219–226.
14. Maurin M, Raoult D (1999) Q fever. *Clin Microbiol Rev* 12: 518–553.
15. Lepidi H, Houpiikian P, Liang Z, Raoult D (2003) Cardiac valves in patients with Q fever endocarditis: microbiological, molecular, and histologic studies. *J Infect Dis* 187: 1097–1106.
16. Izzo AA, Marmion BP (1993) Variation in IFN- γ responses to *Coxiella burnetii* antigens with lymphocytes from vaccinated or naturally infected subjects. *Clin Exp Immunol* 94: 507–515.
17. Ghigo E, Capo C, Tung CH, Raoult D, Gorvel JP, et al. (2002) *Coxiella burnetii* survival in THP-1 monocytes involves the impairment of phagosome maturation: IFN- γ mediates its restoration and bacterial killing. *J Immunol* 169: 4488–4495.
18. Savill J, Dransfield I, Gregory C, Haslett C (2002) A blast from the past: clearance of apoptotic cells regulates immune responses. *Nat Rev Immunol* 2: 965–975.
19. Voll RE, Herrmann M, Roth EA, Stach C, Kalden JR, et al. (1997) Immunosuppressive effects of apoptotic cells. *Nature* 390: 350–351.
20. Mosser DM (2003) The many faces of macrophage activation. *J Leukoc Biol* 73: 209–212.
21. Mantovani A, Sica A, Sozzani S, Allavena P, Vecchi A, et al. (2004) The chemokine system in diverse forms of macrophage activation and polarization. *Trends Immunol* 25: 677–686.
22. Bronte V, Zanovello P (2005) Regulation of immune responses by L-arginine metabolism. *Nat Rev Immunol* 5: 641–654.
23. Hoffmann PR, deCathelineau AM, Ogdan CA, Leverrier Y, Bratton DL, et al. (2001) Phosphatidylserine (PS) induces PS receptor-mediated macrophagocytosis and promotes clearance of apoptotic cells. *J Cell Biol* 155: 649–659.
24. Dellacasagrande J, Ghigo E, Raoult D, Capo C, Mege JL (2002) IFN- γ -induced apoptosis and microbicidal activity in monocytes harboring the intracellular bacterium *Coxiella burnetii* require membrane TNF and homotypic cell adherence. *J Immunol* 169: 6309–6315.
25. Honstetter A, Imbert G, Ghigo E, Gouriet F, Capo C, et al. (2003) Dysregulation of cytokines in acute Q fever: role of interleukin-10 and tumor necrosis factor in chronic evolution of Q fever. *J Infect Dis* 187: 956–962.
26. Ghigo E, Honstetter A, Capo C, Gorvel JP, Raoult D, et al. (2004) Link between impaired maturation of phagosomes and defective *Coxiella burnetii* killing in patients with chronic Q fever. *J Infect Dis* 190: 1767–1772.
27. Tosello-Tramont AC, Brugnera E, Ravichandran KS (2001) Evidence for a conserved role for CRKII and Rac in engulfment of apoptotic cells. *J Biol Chem* 276: 13797–13802.
28. Kinchen JM, Cabello J, Klingele D, Wong K, Feichtinger R, et al. (2005) Two pathways converge at CED-10 to mediate actin rearrangement and corpse removal in *C. elegans*. *Nature* 434: 93–99.
29. Botcher A, Gaipal US, Furnrohr BG, Herrmann M, Girkontaite I, et al. (2006) Involvement of phosphatidylserine, alphavbeta3, CD14, CD36, and complement C1q in the phagocytosis of primary necrotic lymphocytes by macrophages. *Arthritis Rheum* 54: 927–938.
30. Ghigo E, Capo C, Raoult D, Mege JL (2001) Interleukin-10 stimulates *Coxiella burnetii* replication in human monocytes through tumor necrosis factor down-modulation: role in microbicidal defect of Q fever. *Infect Immun* 69: 2345–2352.
31. Zamboni DS, Rabinovitch M (2004) Phagocytosis of apoptotic cells increases the susceptibility of macrophages to infection with *Coxiella burnetii* phase II through down-modulation of nitric oxide production. *Infect Immun* 72: 2075–2080.
32. Freire-de-Lima CG, Nascimento DO, Soares MB, Bozza PT, Castro-Faria-Neto HC, et al. (2000) Uptake of apoptotic cells drives the growth of a pathogenic trypanosome in macrophages. *Nature* 403: 199–203.
33. Van Zandbergen G, Klinger M, Mueller A, Dannenberg S, Gebert A, et al. (2004) Cutting edge: neutrophil granulocyte serves as a vector for *Leishmania* entry into macrophages. *J Immunol* 173: 6521–6525.
34. Byrne A, Reen DJ (2002) Lipopolysaccharide induces rapid production of IL-10 by monocytes in the presence of apoptotic neutrophils. *J Immunol* 168: 1968–1977.
35. Hart SP, Smith JR, Dransfield I (2004) Phagocytosis of opsonized apoptotic cells: roles for 'old-fashioned' receptors for antibody and complement. *Clin Exp Immunol* 135: 181–185.
36. Erwig LP, McPhillips KA, Wynes MW, Ivetic A, Ridley AJ, et al. (2006) Differential regulation of phagosome maturation in macrophages and dendritic cells mediated by Rho GTPases and ezrin-radixin-moesin (ERM) proteins. *Proc Natl Acad Sci U S A* 103: 12825–12830.
37. Jones EA, Flavell RA (2005) Distal enhancer elements transcribe intergenic RNA in the IL-10 family gene cluster. *J Immunol* 175: 7437–7446.
38. Chung EY, Liu J, Homma Y, Zhang Y, Brendolan A, et al. (2007) Interleukin-10 expression in macrophages during phagocytosis of apoptotic cells is mediated by homeodomain proteins Pbx1 and Prep-1. *Immunity* 27: 952–964.
39. Mege JL, Meghari S, Honstetter A, Capo C, Raoult D (2006) The two faces of interleukin-10 in human infectious diseases. *Lancet Infect Dis* 6: 557–569.
40. Oral HB, Kottenko SV, Yilmaz M, Mani O, Zumkehr J, et al. (2006) Regulation of T cells and cytokines by the interleukin-10 (IL-10)-family cytokines IL-19, IL-20, IL-22, IL-24 and IL-26. *Eur J Immunol* 36: 380–388.
41. Capo C, Amirayan N, Ghigo E, Raoult D, Mege JL (1999) Circulating cytokine balance and activation markers of leucocytes in Q fever. *Clin Exp Immunol* 115: 120–123.
42. Strober W, Kelsall B, Fuss I, Marth T, Ludviksson B, et al. (1997) Reciprocal IFN- γ and TGF- β responses regulate the occurrence of mucosal inflammation. *Immunol Today* 18: 61–64.
43. Vodovotz Y, Bogdan C, Paik J, Xie QW, Nathan C (1993) Mechanisms of suppression of macrophage nitric oxide release by transforming growth factor- β . *J Exp Med* 178: 605–613.
44. Tsunawaki S, Sporn M, Ding A, Nathan C (1988) Deactivation of macrophages by transforming growth factor- β . *Nature* 334: 260–262.
45. Gorham JD, Guler ML, Fenoglio D, Gubler U, Murphy KM (1998) Low dose of TGF- β attenuates IL-12 responsiveness in murine Th cells. *J Immunol* 161: 1664–1670.
46. Schmitt E, Hoehn P, Huels C, Goedert S, Palm N, et al. (1994) T helper type 1 development of naive CD4⁺ T cells requires the coordinate action of interleukin-12 and interferon- γ and is inhibited by transforming growth factor- β . *Eur J Immunol* 24: 793–798.
47. Schmidt-Weber CB, Blaser K (2004) Regulation and role of transforming growth factor- β in immune tolerance induction and inflammation. *Curr Opin Immunol* 16: 709–716.
48. Van Heyningen TK, Collins HL, Russell DG (1997) IL-6 produced by macrophages infected with *Mycobacterium* species suppresses T cell responses. *J Immunol* 158: 330–337.
49. Jankovic D, Trinchieri G (2007) IL-10 or not IL-10: that is the question. *Nat Immunol* 8: 1281–1283.
50. Barker RN, Erwig LP, Hill KS, Devine A, Pearce WP, et al. (2002) Antigen presentation by macrophages is enhanced by the uptake of necrotic, but not apoptotic, cells. *Clin Exp Immunol* 127: 220–225.
51. Ip WK, Lau YL (2004) Distinct maturation of, but not migration between, human monocyte-derived dendritic cells upon ingestion of apoptotic cells of early or late phases. *J Immunol* 173: 189–196.
52. Honstetter A, Ghigo E, Moynault A, Capo C, Toman R, et al. (2004) Lipopolysaccharide from *Coxiella burnetii* is involved in bacterial phagocytosis, filamentous actin reorganization, and inflammatory responses through Toll-like receptor 4. *J Immunol* 172: 3695–3703.
53. Meghari S, Honstetter A, Lepidi H, Ryffel B, Raoult D, et al. (2005) TLR2 is necessary to inflammatory response in *Coxiella burnetii* infection. *Ann N Y Acad Sci* 1063: 161–166.
54. Capo C, Lindberg FP, Meconi S, Zaffran Y, Tardei G, et al. (1999) Subversion of monocyte functions by *Coxiella burnetii*: impairment of the cross-talk between $\alpha\beta$ 3 integrin and CR3. *J Immunol* 163: 6078–6085.
55. Fournier PE, Marrie TJ, Raoult D (1998) Diagnosis of Q fever. *J Clin Microbiol* 36: 1823–1834.
56. Holdenrieder S, Stieber P, Chan LY, Geiger S, Kremer A, et al. (2005) Cell-free DNA in serum and plasma: comparison of ELISA and quantitative PCR. *Clin Chem* 51: 1544–1546.
57. Benoit M, Fenollar F, Raoult D, Mege JL (2007) Increased levels of circulating IL-16 and apoptosis markers are related to the activity of Whipple's disease. *PLoS ONE* 2: e494. doi:10.1371/journal.pone.0000494.
58. Desnues B, Raoult D, Mege JL (2005) IL-16 is critical for *Tropheryma whipplei* replication in Whipple's disease. *J Immunol* 175: 4575–4582.
59. Torino PR, Riccio EK, Corte-Real S, Daniel-Ribeiro CT, de Fatima Ferreira-Cruz M (2006) Dexamethasone has pro-apoptotic effects on non-activated fresh peripheral blood mononuclear cells. *Cell Biol Int* 30: 133–137.
60. Meghari S, Berruyer C, Lepidi H, Galland F, Naquet P, et al. (2007) Vanin-1 controls granuloma formation and macrophage polarization in *Coxiella burnetii* infection. *Eur J Immunol* 37: 24–32.
61. Chu JJ, Ng ML (2004) Infectious entry of West Nile virus occurs through a clathrin-mediated endocytic pathway. *J Virol* 78: 10543–10555.
62. Schmittgen TD, Zakrajsek BA, Mills AG, Gorn V, Singer MJ, et al. (2000) Quantitative reverse transcription-polymerase chain reaction to study mRNA decay: comparison of endpoint and real-time methods. *Anal Biochem* 285: 194–204.